

Elastomeric binary phase gratings for measuring acceleration, displacement, strain, and stress

John A. Rogers, Dong Qin, Olivier J. A. Schueller, and George M. Whitesides
Department of Chemistry, Harvard University, Cambridge, Massachusetts 02138

(Received 1 April 1996; accepted for publication 10 June 1996)

This article describes the fabrication and operating principles of a device suitable for measuring displacements, stresses, strains, accelerations, and forces. The device consists of an elastomeric material with a surface relief diffraction grating embossed on its surface. Mechanical compression of this element changes the way that it diffracts light. This article also describes designs and performance characteristics of simple accelerometers and pressure sensors based on these devices.

© 1996 American Institute of Physics. [S0034-6748(96)05109-X]

I. INTRODUCTION

This article describes a new kind of device—an elastomeric element having a relief grating embossed on its surface—for measuring displacements, strains, stresses, forces, and accelerations. In this device, mechanical compression controls the relative optical path of light passing through it. As a result, the optical phase and therefore the pattern of diffraction are coupled to the compression. This report describes the fabrication and operation of the device and illustrates its application in a simple accelerometer and a pressure sensor.

There are many techniques for measuring displacements, strains, stresses, and accelerations. Optical interferometry, one of the most common methods for determining displacements, has sensitivity in the nanometer range.¹ Other methods with sensitivities in the micron and submicron range include measurements of changes in capacitance² and phase-sensitive detection of the reflection of ultrasonic waves.³ Stresses and strains can be determined by changes in the birefringence of strongly photoelastic samples caused by deformation.⁴ Surface strains can be determined by measuring the change in wavelength of a diffraction grating attached to the sample.⁵ Characteristics such as ease of use and fabrication, low cost, and insensitivity to optical alignment make the elastomeric phase gratings described in this article an attractive alternative to these other methods.

This article is organized into five parts: (i) We begin in the theory section with a brief, qualitative description of how light diffracts from the gratings before and during compression. (ii) We present a simple analytical model that describes the optical properties of the elastomeric binary phase gratings as they are compressed. Finite element modeling identifies the limitations of this model. (iii) We describe the fabrication of the gratings and present results obtained from gratings in different optical configurations. (iv) In the experimental section, we describe the design and performance of an accelerometer and a pressure sensor that are based on compression of an elastomeric binary phase grating. (v) Finally, in the results and discussion section, we compare the experimental results to computations.

II. THEORY

A. Qualitative description of the elastomeric binary phase grating

Sensors based on elastomeric binary phase gratings operate by simple principles. The gratings have relief structure on their surface that diffracts light passing through or reflecting from them. The period of the grating determines the separation of the diffracted orders, and the depth of the surface relief determines their relative intensities. Compressing the grating in the out-of-plane direction reduces the depth of the surface relief and changes the intensity of each of the diffracted orders. Figure 1 shows one possible means for achieving the compression, the mechanical response of the grating to this compression, and one possible configuration for generating diffracted light. The change in intensity of the diffracted orders induced by compression is large (>17 dB), and can be related quantitatively to the degree of compression. The relationship between the change in intensity of the diffracted orders and the mechanical compression is the focus of the next three sections.

B. Optical response

To provide a semiquantitative understanding of the optical behavior of the binary elastomeric phase grating, we develop a simple model to compute the diffraction pattern as a function of the index of refraction of the elastomer and the surroundings, and of the depth of the surface relief. Figure 2 illustrates the coordinate system. We assume that the optical field has infinite extent along x and y , and that there are an infinite number of grating lines extending infinitely and oriented along the y axis. In this case, the optical field just after the grating ($z=0^-$) is related to the optical field just before the grating ($z=0^+$) by

$$E(x, z=0^-) = E(z=0^+) \tau(x), \quad (1)$$

where $\tau(x)$ is the transmission function of the grating. The Fraunhofer diffraction pattern $E(x', z')$ is given by the Fourier transformation of the transmission function, $\tau(x)$, evaluated at the spatial frequency $x'/\lambda z'$, where λ is the wavelength of the light.^{6,7}

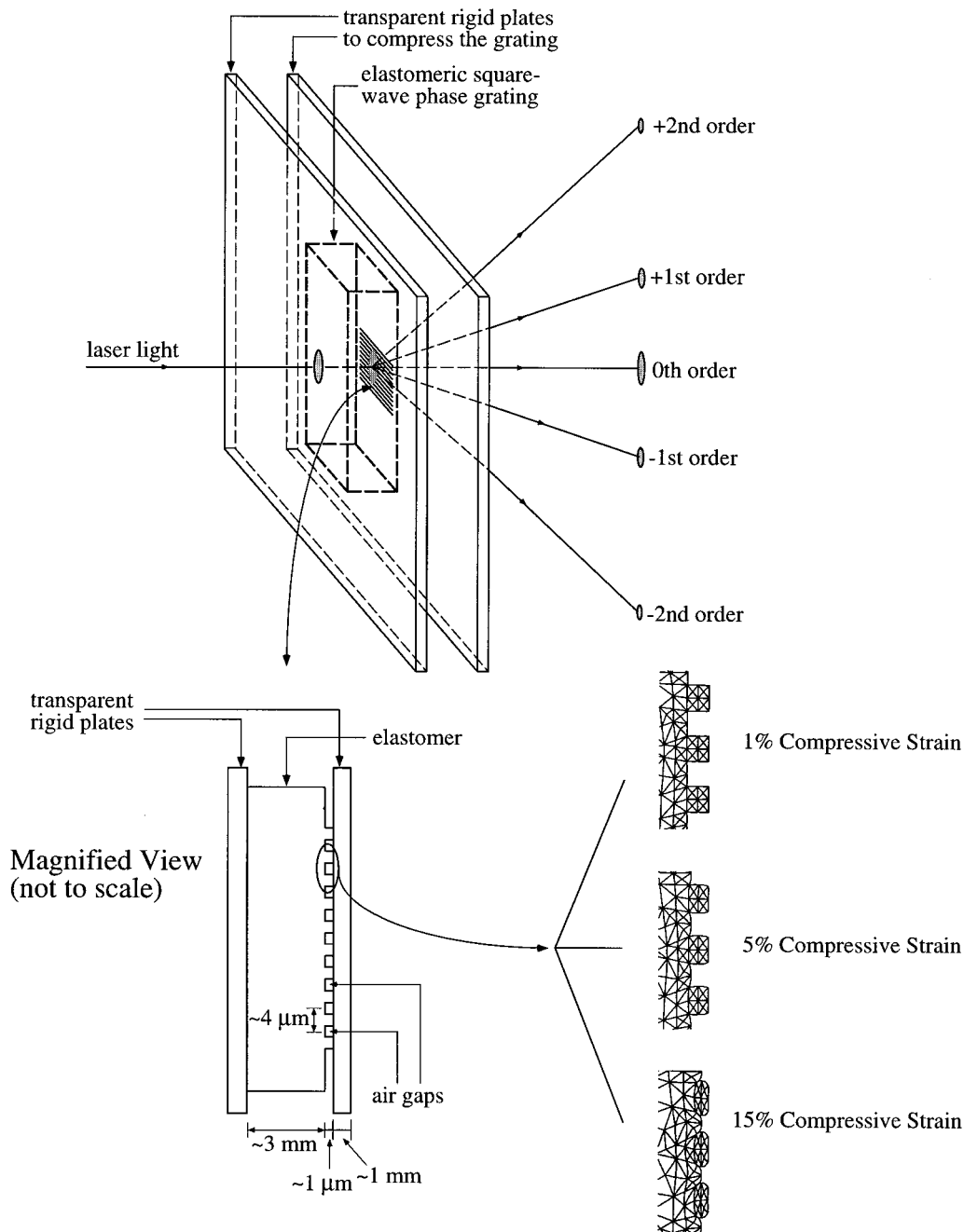


FIG. 1. An elastomeric element with a surface relief grating is compressed between two optically transparent rigid plates. Pressure applied to the plates compresses the grating, thereby decreasing the relief of the grating. This change in relief alters, in a well-defined manner, the way that light diffracts from the grating. Finite-element modeling illustrates how the structure of the surface relief changes with the strain.

For present purposes, we assume that the transmission function is binary and remains so during compression. For a grating with equal linewidths and spaces,

$$\tau(x) = \begin{cases} e^{i\varphi} & 2nL < x < (2n+1)L \quad n \in I \\ 1 & \text{otherwise} \end{cases}, \quad (2)$$

where φ is the depth of modulation of the phase, and L is the width and spacing of the lines of the grating. The magnitude of φ depends on the initial depth of the surface relief, the index of refraction of the elastomer and the surroundings (air in this case), and on the degree of compression. If the surface

relief of the grating is in contact with a reflective surface, and the diffraction pattern is monitored in reflection, then Eq. (2) must be modified by replacing φ with 2φ . Figure 3 shows calculated diffraction patterns for $\varphi=0, \pi/4, \pi/2, 3\pi/4$, and π .

The configuration for diffracting light from a grating determines how rapidly the diffraction pattern changes as the depth of surface relief changes. By using the reflection configuration described above, or by passing light through the grating multiple times, the sensitivity of the diffraction pattern to changes in relief can be increased relative to that

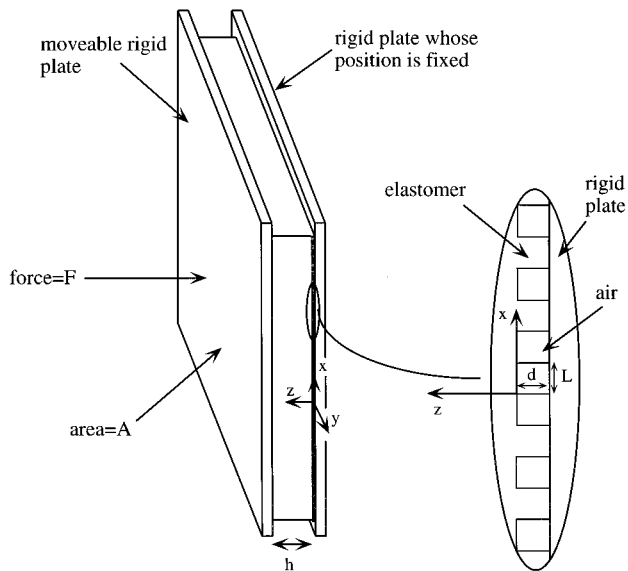


FIG. 2. Definition of axes and geometrical quantities for optical and mechanical calculations.

achieved by passing light through the grating once. In particular, after n passes through the grating, the intensity of the zeroth order beam is given by

$$I_0^{(n)} \propto R^n, \quad (3)$$

where R represents the efficiency of diffraction into the zeroth order for a single pass. Figure 4 illustrates the intensity of the zeroth order diffracted beam as a function of the depth of modulation of the optical phase for one, two, and four passes through a binary grating. Figure 4 also illustrates the response expected for operation in the reflection configuration.

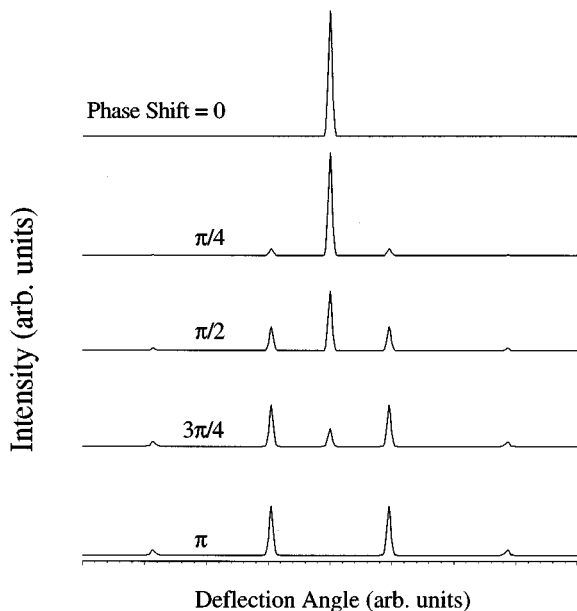


FIG. 3. Diffraction pattern generated by passage of light through a binary phase grating as the depth of modulation of the phase is varied from 0 to π radians in increments of $\pi/4$.

C. Mechanical response and coupling to the optical response

This section models the response of the optical phase φ [Eq. (2)], to compression. The model describes how the optical phase depends on the geometry of the grating and how the grating moves during compression. Accurate determination of the material displacements and the phase requires a treatment of the mechanics that explicitly includes the surface relief structure. Although such a treatment is beyond the scope of a simple analytical description, a semiquantitative understanding can be obtained by examining displacements in a body without a surface relief grating, and by assuming that the binary shape of the surface of the uncompressed grating remains unchanged during the compression. Finite element calculations described in the next section illustrate the exact (linear) behavior of the elastomeric grating upon compression.

Figure 2 defines the coordinate system. For linear elastic materials, a uniform axial stress ($T_{zz} = F/A$, where F is the force perpendicular to the surface of the plates used for compression and A is the area of the elastomeric element) produces a uniform axial strain (ϵ_{zz}) given by

$$T_{zz} = -E\epsilon_{zz}, \quad (4)$$

where E is the Young's modulus. T_{zz} also causes expansions in the x and y directions. These expansions are related to the magnitude of the compression along z and the Poisson's ratio (σ) by

$$\epsilon_{xx} = \epsilon_{yy} = -\sigma\epsilon_{zz}. \quad (5)$$

Equations (4) and (5) determine displacements throughout the material. These displacements are given by

$$u_x(x, y, z) = \frac{\sigma T_{zz}}{E} x, \quad (6)$$

$$u_y(x, y, z) = \frac{\sigma T_{zz}}{E} y, \quad (7)$$

$$u_z(x, y, z) = -\frac{T_{zz}}{E} z. \quad (8)$$

The change in the depth of the modulation of the optical phase $\Delta\varphi$ can be defined as

$$\Delta\varphi = \varphi_0 - \varphi_1, \quad (9)$$

where φ_0 is the depth of modulation of the phase associated with the uncompressed grating and φ_1 is that associated with the compressed grating. These phases are related to the uncompressed (d_0) and compressed (d_1) depths of surface relief by

$$\begin{aligned} \Delta\varphi &= \frac{2\pi}{\lambda} (n_e - n_a)d_0 - \frac{2\pi}{\lambda} (n_e - n_a)d_1 \\ &= \frac{2\pi}{\lambda} (n_e - n_a)(d_0 - d_1), \end{aligned} \quad (10)$$

where n_e and n_a are the indices of refraction for the elastomer and the air, respectively, and λ is the wavelength of light.

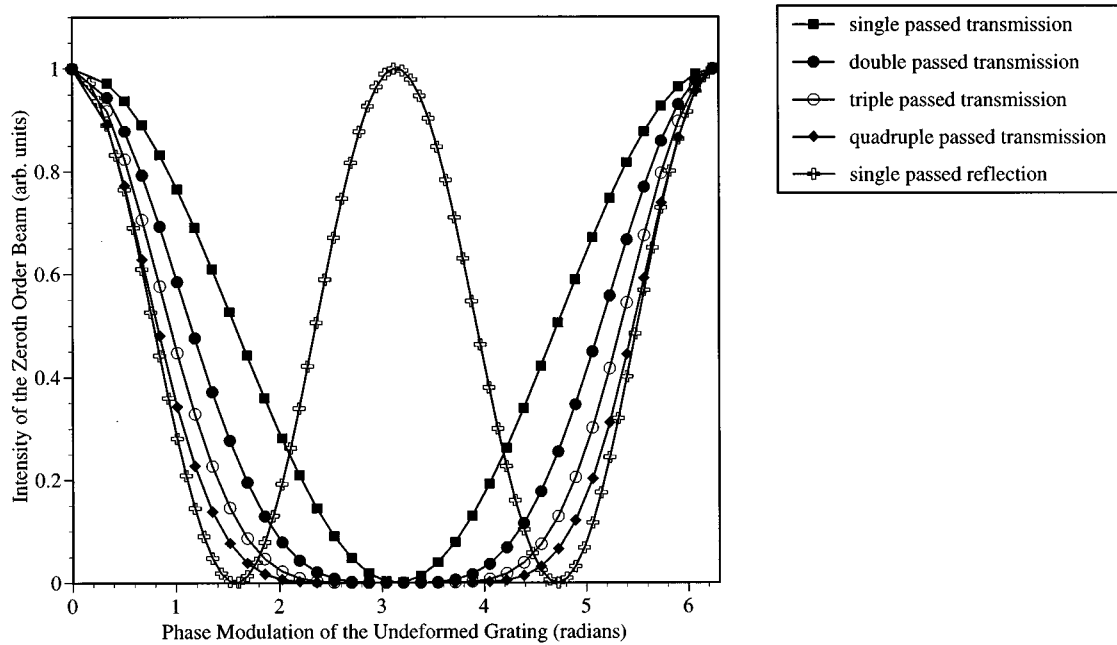


FIG. 4. Calculations of the intensity of the zeroth order diffracted beam generated by passage through or reflection from a binary grating. The rate of change of the zeroth order intensity increases as the number of passages of light through the grating increases. Reflection from the grating effectively increases the depth of modulation of the phase by a factor of 2.

For small compressions, we expect that the change in the depth of the surface relief ($d_0 - d_1$) is approximately linearly related to the z displacement of an element with a flat surface at a depth equal to the depth of the uncompressed relief

$$d_1 - d_0 \propto u_z(z = d_0). \quad (11)$$

With this relation

$$\Delta \varphi \propto u_z(z = d_0) = \frac{-T_{zz}d_0}{E} = \frac{-Fd_0}{AE}. \quad (12)$$

Using the relationship between the stress and strain, and the definitions of these quantities

$$T_{zz} = \frac{F}{A} = -E\epsilon_{zz} = -E \frac{\Delta h}{h} \quad (13)$$

and Eq. (12) can be rewritten as

$$\Delta \varphi \propto \frac{-d_0 \Delta h}{h} = -d_0 \epsilon_{zz}, \quad (14)$$

where Δh is the distance of compression, and h is the undeformed thickness of the elastomer.

D. Response time

The resonance frequency for out-of-plane compressions determines the response time of the grating. The relevant equation of motion (neglecting damping) is

$$\frac{\partial^2 u_z}{\partial t^2} = \frac{E}{\rho} \frac{\partial^2 u_z}{\partial z^2}. \quad (15)$$

Solutions to this equation show that, for a grating element of thickness h and density ρ , the resonant frequency for the out-of-plane breathing mode of motion is

$$\nu = \frac{1}{4h} \left(\frac{E}{\rho} \right)^{1/2}. \quad (16)$$

For typical elastomeric materials⁸ ($E \sim 2-3$ MPa and $\rho \sim 1500$ kg/m³) this frequency is in the kHz range for gratings with thicknesses < 1 cm, and in the MHz range for thicknesses < 10 μ m.

E. Finite-element modeling: Inadequacies of the simple model

The simple mechanical and optical model described above neglects much of what happens when the grating is compressed. Finite-element calculations show how the grating actually deforms. (The calculations were performed in the plane-strain approximation. We assumed that the grating element sticks well to the plates used for compression, so that lateral displacements at the top and bottom of the element were zero. Stress-free boundary conditions were used at the sides of the element, and the load was applied perpendicular to the surfaces. All calculations were performed in the linear regime, with a Poisson's ratio of 0.45.) Figure 5 illustrates the deformed finite element meshes at four different strains typical of those examined experimentally. Figure 5 shows that the grating does not maintain a binary shape during the compression. Deviations arising from bending of the relief pillars will be most pronounced for gratings with depths of surface relief that are considerably larger than the period of the grating. Deviations arising from "sagging" of the recessed regions will be most pronounced for gratings with depths of surface relief that are considerably smaller than the period of the grating. As we will show in the results

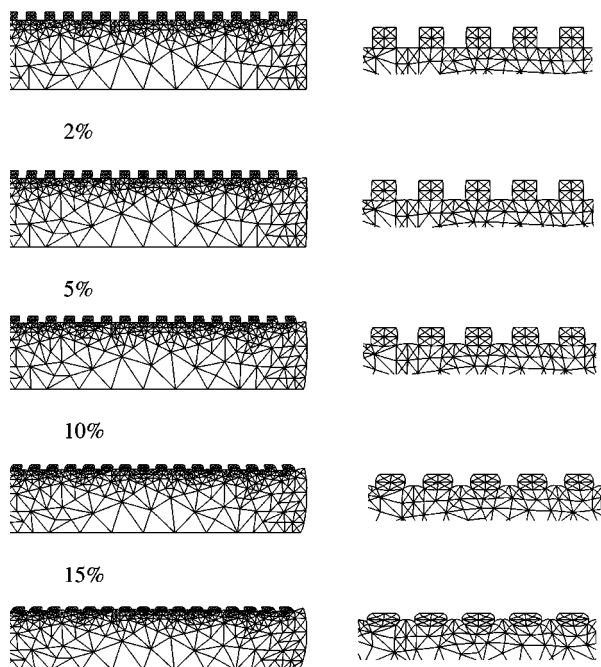


FIG. 5. Finite-element calculations of the deformation of an elastomeric binary phase grating caused by compression. The distorted finite-element mesh is illustrated at strains of 1%, 2%, 5%, 10%, and 15%. These simulations indicate that compressions induce deviations from a square wave shape.

and discussion section, for the gratings examined here, the simple analytical model accounts for most of the important optical characteristics.

III. EXPERIMENT

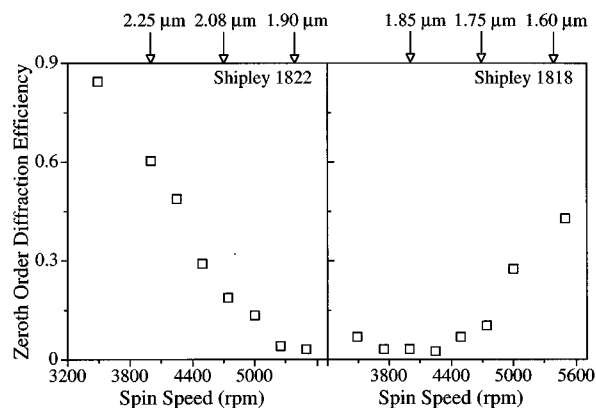
In this section, we describe the fabrication of elastomeric binary phase gratings. We also demonstrate their optical response and how this response changes during compression. Finally, we describe the design and operation of two devices, an accelerometer and a pressure sensor.

A. Fabrication of elastomeric binary phase gratings

Binary elastomeric phase gratings were fabricated by casting poly-dimethylsiloxane (PDMS) over photolithographically patterned photoresist on silicon. Once cured, the PDMS was removed from the photoresist, leaving a relief structure with the geometry of the patterned photoresist embossed on its surface. The spin speed for application of the photoresist, and the photolithography determined the dimensions of the pattern. For the binary gratings studied here, the thickness of the photoresist was between 1 and 2 μm , and the pattern consisted of two micron lines separated by two microns. The thickness of the PDMS was between 0.5 and 5 mm.

B. Optical properties of the uncompressed gratings

A series of binary phase gratings with different depths of surface relief were produced following the procedure described in the preceding section. Figure 6 illustrates how



Decreasing Thickness --->

FIG. 6. Zeroth order diffraction efficiencies for green light diffracted from uncompressed elastomeric binary phase gratings as a function of the spin speed and thickness of the photoresist from which the grating was cast. The data include gratings cast from two different formulations of photoresist: Shipley 1818 and 1822.

these gratings diffract light out of the zeroth order beam. As the spin speed for applying the photoresist changes, the depth of surface relief and the diffraction properties of the gratings change. As Fig. 6 indicates, changes in the depth of surface relief by fractions of a micron induce large changes in the intensity of the zeroth order diffracted beam. This sensitivity to the depth of surface relief provides the basis for a device that is sensitive to dimensional changes caused by compression or other mechanisms.

C. Optical response during mechanical compression

To determine how the optical response of the elastomeric grating is related to mechanical compression and to the dimensions of the grating, we performed measurements with gratings having different geometries. Figure 7 illustrates the different configurations for the measurements, and introduces terminology that is used throughout the remainder of this article. We note that compression of all of the gratings was reversible and reproducible during the several hundred cycles of compression investigated in this study.

1. The effect of physical properties on the optical response

To illustrate the ability to change the pattern of diffraction reversibly by mechanically compressing an elastomeric phase grating, a 3.0-mm-thick grating with 1.2 μm deep relief on its surface was compressed in the out-of-plane direction by mounting the grating between microscope slides attached to mirror mounts on calibrated translation stages. Using the transmission configuration, the efficiencies for diffraction of red (He-Ne) and green (Ar^+) laser light into the zeroth and first orders were measured with a photodiode as a function of displacement (Fig. 8). Approximately 15% strain switched the grating from efficient transmission to strong diffraction. As the data show, for strains of this magnitude, the compression is elastic, and therefore reversible. (The solid lines in Fig. 8 indicate computations using the simple

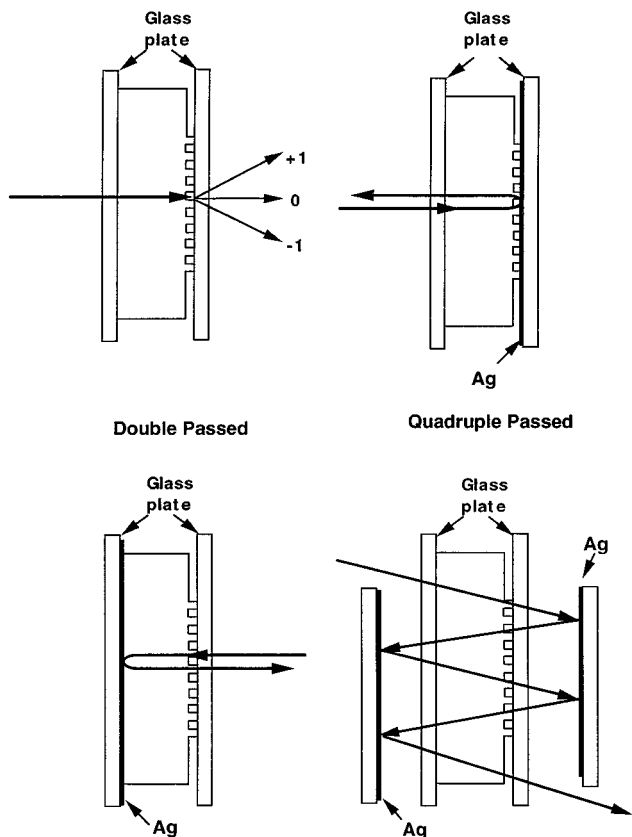


FIG. 7. Schematic illustrations of the different configurations used for measuring the optical response of the elastomeric gratings. The terminology introduced in this figure is used throughout the article.

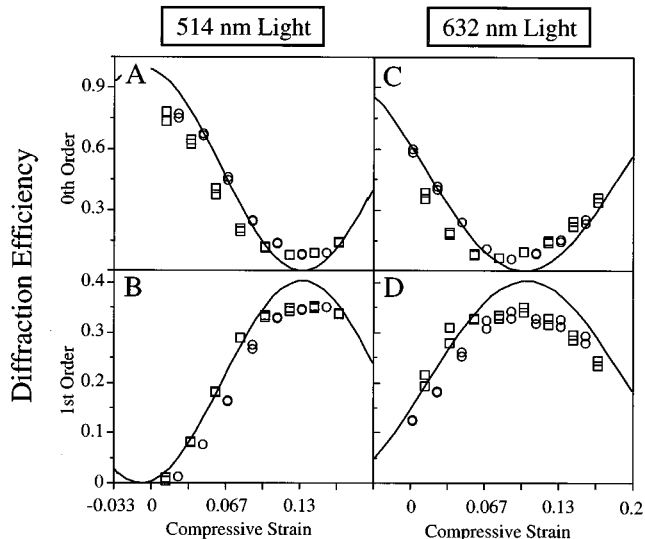


FIG. 8. Diffraction efficiencies measured (\square during compressing; \circ during releasing) and calculated (solid lines) for a binary elastomeric phase grating as a function of compressive strain. (A and B) are, respectively, diffraction efficiencies of the zeroth and first order beams using 514 nm laser light. (C and D) are, respectively, efficiencies for diffraction into the zeroth and first order beams using 632 nm laser light. Data represented by squares and circles were collected during two cycles of compression and release, respectively.

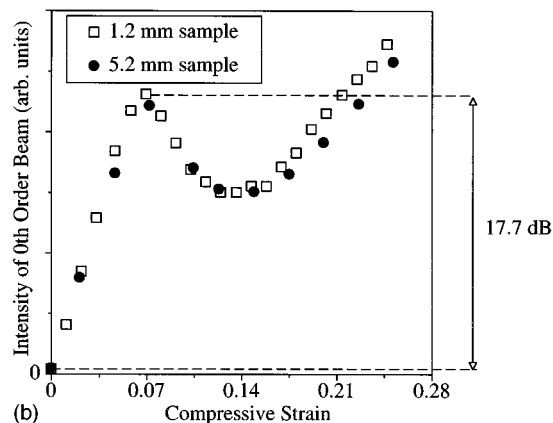
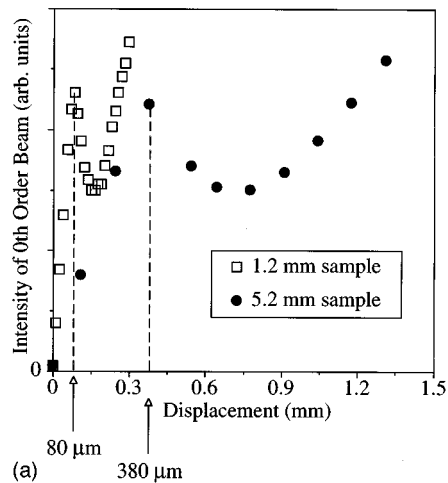


FIG. 9. Intensity of the zeroth order beam generated from passage of 514 nm light through 1.2- and 5.2-mm-thick elastomeric gratings with 1.8- μ m-deep surface relief (a) as a function of displacement and (b) as a function of strain of the rigid plates used to perform the compression. These results indicate that the change of the intensity of the zeroth order beam depends on the strain.

model described in the theory section. The results and discussion section describes these computations in detail.)

To investigate how the response of the grating changes with the overall thickness of the elastomer, 5.2- and 1.2-mm-thick gratings with 1.8 μ m deep surface relief were compressed and the intensity of the zeroth order beam was recorded in the transmission configuration as a function of the compressive displacement (Fig. 9). Qualitatively, these data indicate that the response of the grating is a function of the strain. They also indicate that for a given surface relief structure, the sensitivity to displacement increases as the overall thickness of the grating decreases.

To characterize how the response of the grating changes with the uncompressed depth of surface relief, 5.2- and 4.9-mm-thick gratings with 1.8 and 1.2- μ m-deep relief structure, respectively, were compressed and the intensities of the zeroth order beams were recorded as a function of displacement. Measurements were made using the transmission configuration (Fig. 10). These data show that for a given thickness, the sensitivity to displacements and to strains increases as the depth of the surface relief structure increases.

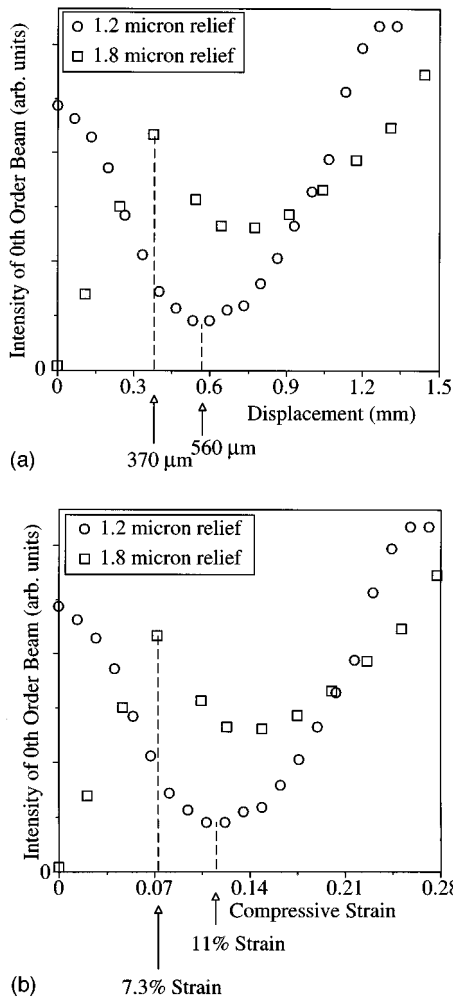


FIG. 10. Intensity of the zeroth order beam generated from passage of 514 nm light through 4.9- and 5.2-mm-thick elastomeric gratings with 1.2- and 1.8- μm -deep surface relief, respectively, (a) as a function of displacement and (b) as a function of strain of the rigid plates used to perform the compression. These results indicate that the sensitivity of the intensity of the zeroth order beam to displacement and strain depends on the initial depth of surface relief.

2. The effect of the configuration of the optical probe on the response

To understand how the optical arrangement changes the response of the grating, a 4.9-mm-thick grating with 1.2 μm relief was compressed between transparent and reflective plates and the intensity of the zeroth order beam was measured as a function of displacement. These measurements were made once with the relief structure in contact with the reflective plate and once with the relief structure in contact with the transparent plate [Fig. 11(A)]. The data indicate that the sensitivity to displacements is higher in the reflection or the double passed configurations than in the transmission configuration.

In a second experiment, a 4.9-mm-thick grating with 1.2 μm relief was compressed and the intensity of the zeroth order beam generated from four passes through the grating was measured as a function of displacement [Fig. 11(B)]. The data indicate that the sensitivity to displacements is

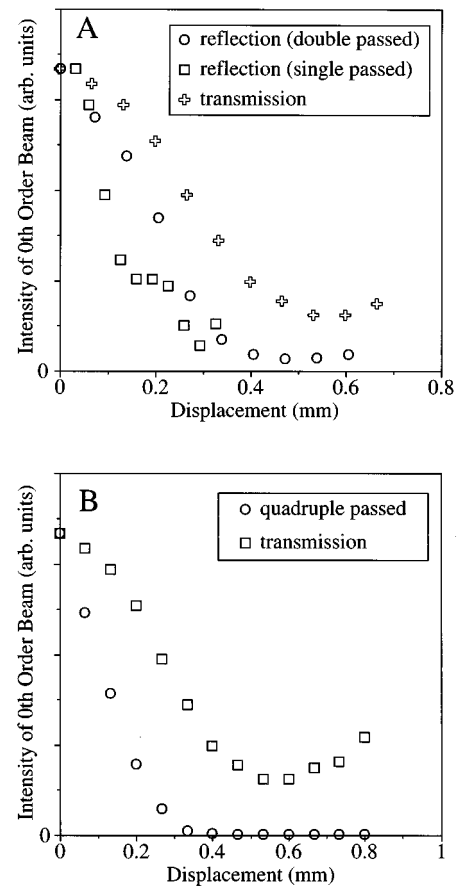


FIG. 11. (A) Intensity of the zeroth order beam generated in the transmission, reflection and double passed configurations with 514 nm light and a 4.9-mm-thick elastomeric grating with 1.2- μm -deep surface relief as a function of the displacement of the rigid plates used to perform the compression. (B) Intensity of the zeroth order beam generated in the transmission and quadruple passed configurations with 514 nm light and a 4.9-mm-thick elastomeric grating with 1.2- μm -deep surface relief as a function of the displacement of the rigid plates used to perform the compression.

higher in the quadruple passed configuration than it is in the transmission configuration.

D. Examples of devices based on elastomeric binary phase gratings

1. A simple accelerometer

To illustrate one application of the elastomeric grating, we constructed a simple device to measure accelerations. In this accelerometer, a mass mounted on a freely moving piston is connected to a reflective rigid plate that is attached to one side of the grating. The other side of the grating is attached to a transparent rigid support (Fig. 12). An acceleration of this device along the direction that the piston can move compresses the grating and changes the intensity of the zeroth order diffracted beam. This change in intensity can be related to the magnitude of the acceleration. Since we did not have a simple means to subject the device to controlled accelerations, we mounted the accelerometer in a vertical configuration and varied the mass. Figure 13 shows the results of these measurements. These data indicate that the response is sensitive to the mass (acceleration) and scales with the com-

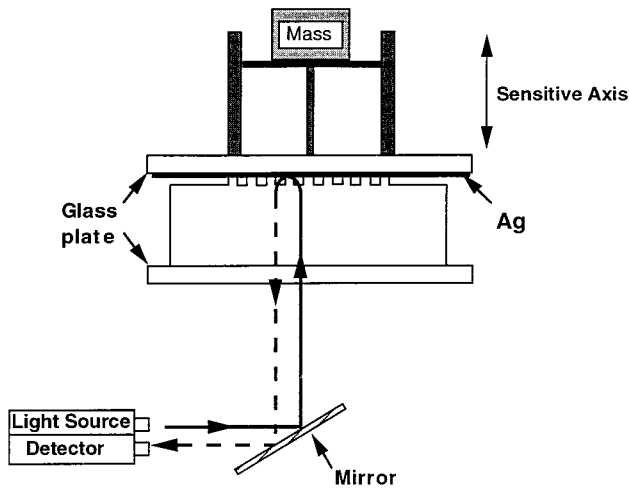


FIG. 12. Schematic illustration of an accelerometer based on an elastomeric binary phase grating. Upon acceleration, the mass compresses the grating and changes the way that light is diffracted. This change is related to the magnitude of the acceleration.

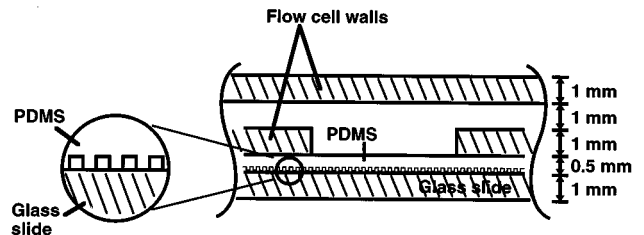
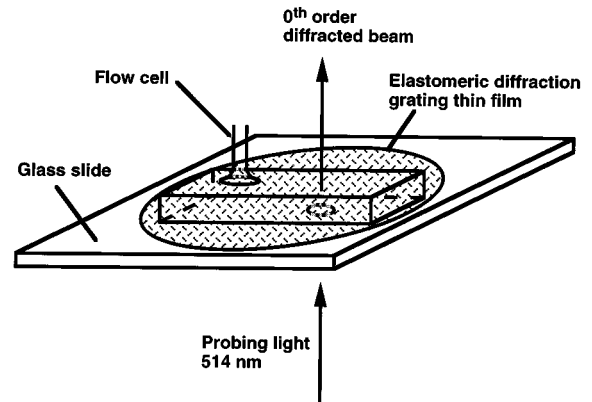


FIG. 14. Schematic illustration of a pressure sensor based on an elastomeric binary phase grating. Fluid pressure from the inside of the flow cell compresses the thin grating against a glass slide.

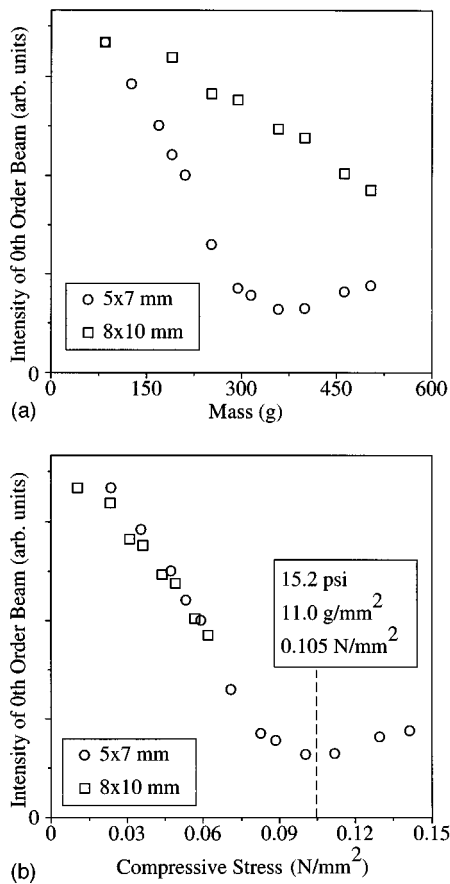


FIG. 13. Intensity of the zeroth order beam generated from passage of 514 nm light through 4.9-mm-thick elastomeric gratings with 1.2- μm -deep surface relief with lateral dimensions 5 \times 7 and 8 \times 10 mm (a) as a function of the mass used to compress the grating and (b) as a function of compressive stress generated by the mass. These results indicate that the change in zeroth order beam intensity depends on the stress.

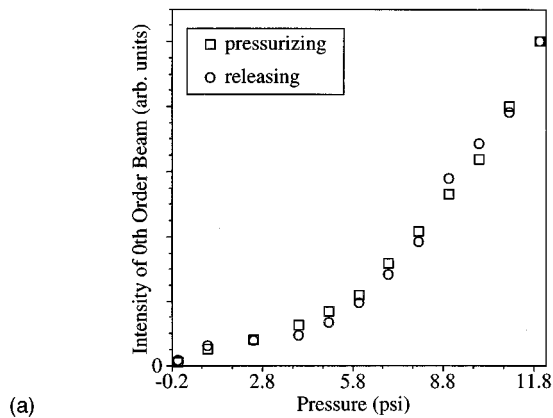
pressive stress. As a result, the lateral dimensions of the elastomeric grating and the mass can be varied to adjust the range of sensitivity to accelerations.

2. A simple pressure sensor

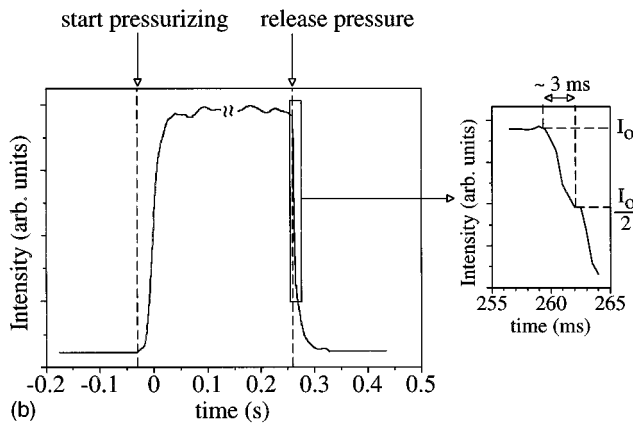
We also fabricated a device sensitive to pressure changes. A thin (~ 0.5 mm) grating covering an opening (2 mm in diameter) in a flow cell formed the basis of the device. The surface relief of the grating was oriented away from the opening in the flow cell, and was held tightly against a glass slide. Pressure inside the cell compressed the grating against the glass slide, and changed the pattern of diffraction. Figure 14 schematically illustrates the device. To characterize the device, the flow cell was connected to the regulator of a high-pressure nitrogen tank. We measured the intensity of the zeroth order diffracted beam as a function of applied nitrogen pressure [Fig. 15(a)]. Pressurizing the flow cell with water produced similar results. Figure 15(b) illustrates the transient response.

IV. RESULTS AND DISCUSSION

This section shows that the simple mechanical and optical analysis introduced in the theory section accounts for many features of the data. First, consider the data illustrated in Fig. 8. Results from the theory section [Eqs. (2) and (14)] determine efficiencies for diffraction into the various orders as a function of the strain, given the constant of proportionality between strain and optical phase. By fitting the dependence of the intensity of the 514 nm first order diffracted light on the compressive strain to computations using Eqs.



(a)



(b)

FIG. 15. (a) Intensity of the zeroth order beam generated from passage of 514 nm light through an elastomeric grating as a function of applied pressure. The results provide a calibration relating the intensity to the pressure. (b) Intensity of the zeroth order beam generated from passage of 514 nm light through an elastomeric grating as a function of time during an increase in pressure and during its release. The fall time is on the order of milliseconds.

(1), (2), and (14), we determined this constant of proportionality. With this constant, we computed the intensities of the other diffracted orders (for both 514 and 633 nm light) as a function of strain. The solid lines in Fig. 8 illustrate the results. The calculations show good agreement with the data.

Other measurements also show agreement with the simple mechanical and optical model. For example, Fig. 9 shows that diffraction patterns from gratings with different thicknesses have the same dependence on the strain. This result is consistent with Eq. (14). Next, according to Eqs. (12) or (14), the ratio of the strains required to induce a change in phase, $\Delta\varphi$, with gratings having different uncompressed depths of surface relief, d_0 , should be equal to the ratio of the depths d_0 . Figure 10 shows that, in agreement with this prediction, the ratio of strains that cause $\Delta\varphi \sim \pi$ is 1.5 ± 0.1 , while the ratio of undeformed surface relief depths is 1.5 ± 0.1 . Finally, as Fig. 13 illustrates, the diffraction properties scale with the compressive stress, rather than the compressive force, an intuitive result consistent with a linear relation between the stress and the strain.

The optical analysis included predictions for the behavior of the device when operated in each of the modes illus-

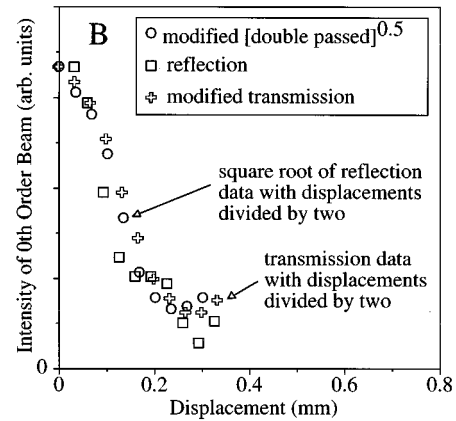
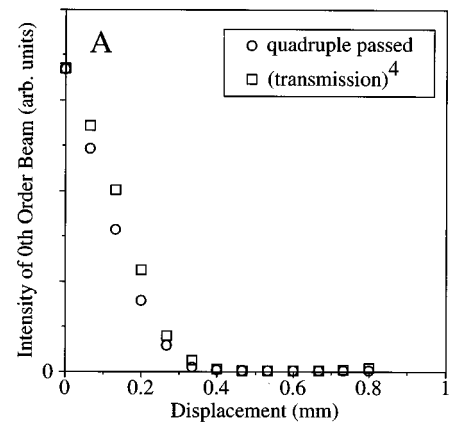


FIG. 16. (A) Fourth power of the intensity of the zeroth order beam generated from transmission of 514 nm light through a 4.9-mm-thick elastomeric grating with 1.2- μm -deep surface relief, and the intensity of the zeroth order beam generated from quadruple passed 514 nm light through a 4.9-mm-thick elastomeric grating with 1.2- μm -deep surface relief as functions of the displacement of the rigid plates used to perform the compression. Figure 16 illustrates that the intensity of the zeroth order beam scales as expected from Eq. (3). (B) Intensity of the zeroth order beam generated from transmission of 514 nm light through a 4.9-mm-thick elastomeric grating with 1.2- μm -deep surface relief as a function of one half of the displacement of the rigid plates used to perform the compression, and the square root of the intensity of the zeroth order beam generated in the double passed configuration with 514 nm light and a 4.9-mm-thick elastomeric grating with 1.2- μm -deep surface relief as a function of one-half of the displacement of the rigid plates used to perform the compression, and the intensity of the zeroth order beam generated in the reflection configuration with 514 nm light and a 4.9-mm-thick elastomeric grating with 1.2- μm -deep surface relief as a function of the displacement of the rigid plates used to perform the compression. Figure 16 illustrates that the intensity of the zeroth order beam scales as expected from results from Sec. III D 1.

trated in Fig. 7. As Fig. 16 shows, when the data are scaled appropriately [optical analysis section, Fig. 11, and Eq. (3)], measurements made in different configurations yield the same results.

The theory section showed that the response time of the grating depends on the Young's modulus, the density, and the thickness of the grating, and is less than 1 ms for gratings made from PDMS with thicknesses less than 1 cm. Measurements illustrated in Fig. 15 indicate a response time that is longer than the predicted value by about a factor of 10. We believe that the discrepancy arises partly from the elastomeric nature of the tubing and other components that connect

the pressure sensor to the high-pressure nitrogen tank.

Finally, we note that, although the theory accurately describes the behavior of the device, there are limitations and some of these were described. For many applications, an empirical characterization, rather than a detailed theory, will be sufficient.

ACKNOWLEDGMENTS

This research was supported in part by the National Science Foundation (PHY-9312572). It also used MRSEC Shared Facilities supported by the NSF under Award No. DMR-9400396. We extend our thanks to Professor Keith Nelson, M.I.T., for the use of lasers and optics laboratories.

J.A.R. gratefully acknowledges funding from the Harvard University Society of Fellows.

- ¹S. Hosoe, *Precision Eng. J. Am. Soc. Precision Eng.* **17**, 258 (1995).
- ²M. H. W. Bonse, C. Mul, and J. W. Spronck, *Sens. Actuators A* **46–47**, 266 (1995).
- ³A. Alsabbah and P. A. Gaydecki, *Measure Sci. Technol.* **6**, 1068 (1995).
- ⁴Y. Niitsu, K. Ichinose, and K. Ikegami, *J. Soc. Mech. Eng., Int. J. Ser. A—Mech. Mater. Eng.* **38**, 68 (1995).
- ⁵P. M. Boone, *Exp. Mech.* Nov. 1971, p. 481.
- ⁶M. V. Klein, *Optics* (Wiley, New York, 1970).
- ⁷J. W. Goodman, *Introduction to Fourier Optics* (McGraw-Hill, New York, 1968).
- ⁸J. Brandup and E. H. Immergut, *Polymer Handbook*, 3rd ed. (Wiley-Interscience, New York, 1989), Vols. 7–13.